https://doi.org/10.31925/farmacia.2026.1.19 **ORIGINAL ARTICLE**

IN VITRO AND *IN OVO* ASSESSMENT OF LABETALOL AND SILIBININ, ALONE AND IN COMBINATION, IN H9C2(2-1) CARDIOMYOCYTE CELLS

RADU PETROMAN [1#], IASMINA-ALEXANDRA PREDESCU [2,3,4#], GABRIELA-FLORENTINA ȚAPOȘ [2,5]*, DANIELA SAȘCO [3], ALINA ANTON [3,4], CONSTANTIN TUDOR LUCA [6,7,8], SILVIA LUCA [6,7,8], SIMINA CRIȘAN [6,7,8], MIHAELA-CRISTINA NEGRU [9], CASIANA BORU [10]

[1]*Department of Rehabilitation, Physical Medicine and Rheumatology, Research Center for Assessment of Human Motion, Functionality and Disability, "Victor Babes" University of Medicine and Pharmacy Timisoara, 300041 Timisoara, Romania*
[2]*Doctoral School, "Victor Babes" University of Medicine and Pharmacy, 2nd Eftimie Murgu Square, 300041 Timisoara, Romania*
[3]*Faculty of Pharmacy, "Victor Babeș" University of Medicine and Pharmacy Timișoara, 2nd Eftimie Murgu Square, 300041, Timișoara, Romania*
[4]*Research Centre for Pharmaco-Toxicological Evaluations, "Victor Babeș" University of Medicine and Pharmacy Timișoara, 2nd Eftimie Murgu Square, 300041, Timișoara, Romania*
[5]*Arad County Clinical Emergency Hospital, 310037, Arad, Romania*
[6]*Cardiology Department, "Victor Babes" University of Medicine and Pharmacy, 2nd Eftimie Murgu Square, 300041 Timisoara, Romania*
[7]*Research Center of the Institute of Cardiovascular Diseases Timisoara, 300310, Timisoara, Romania*
[8]*Institute of Cardiovascular Diseases Timisoara, 300310, Timisoara, Romania*
[9]*Department of ENT, "Victor Babeş" University of Medicine and Pharmacy Timisoara, 2nd Eftimie Murgu Square, 300041, Timișoara, Romania*
[10]*Faculty of Medicine, "Vasile Goldiș" Western University of Arad, 94 Revoluției Blvd., 310130, Arad, Romania*

**corresponding author: gabriela.tapos@umft.ro*
[#]*Authors with equal contribution.*

Manuscript received: December 2025

Abstract

Cardiovascular diseases, particularly ischemic heart disease and angina pectoris, remain a major health problem worldwide. Combining conventional cardiovascular drugs with antioxidant compounds may offer complementary benefits, but biosafety must be carefully evaluated. This study aimed to assess the *in vitro* and *in ovo* biosafety of labetalol (LB; 20-500 nM) and silibinin (SIL; 5-200 µM), administered individually and in combination, using H9c2(2-1) cells and the chorioallantoic membrane model. After 24 h, cell viability, morphology, lysosomal and membrane integrity, and mitochondrial and nuclear morphology were evaluated using MTT, Neutral Red uptake, fluorescence staining, and AO/PI assays. In addition, irritation potential was assessed using the HET-CAM assay. The results showed that cell viability remained comparable to control following all treatments. Mitochondrial and nuclear analyses indicated that organelle structure and morphology were preserved. Furthermore, AO/PI staining revealed no significant induction of apoptosis or necrosis. The HET-CAM assay confirmed the absence of vascular irritation for the tested combination. Overall, the combined administration of LB and SIL did not cause additional cytotoxicity or irritation compared with the individual treatments, supporting the biosafety of this combination.

Rezumat

Bolile cardiovasculare, în special cardiopatia ischemică și angina pectorală, rămân o problemă majoră de sănătate la nivel mondial. Combinarea medicamentelor cardiovasculare convenționale cu compuși antioxidanți poate oferi beneficii complementare, dar biosecuritatea trebuie evaluată cu atenție. Scopul acestui studiu a fost de a evalua biosecuritatea *in vitro* și *in ovo* a labetalolului (LB; 20-500 nM) și a silibininei (SIL; 5-200 µM), administrate individual și în combinație, utilizând celule H9c2(2-1) și modelul membranei corioalantoidiene. După 24 de ore, viabilitatea celulară, morfologia, integritatea lizozomală și membranară, precum și morfologia mitocondrială și nucleară au fost evaluate utilizând MTT, absorbția roșului neutru, colorarea cu fluorescență și testele AO/PI. În plus, potențialul de iritare a fost evaluat utilizând testul HET-CAM. Rezultatele au arătat că viabilitatea celulară a rămas comparabilă cu cea a martorului după toate tratamentele. Analizele mitocondriale și nucleare au indicat conservarea structurii și morfologiei organitelor. Mai mult, colorarea AO/PI nu a relevat nicio inducție semnificativă de apoptoză sau necroză. Testul HET-CAM a confirmat absența iritației vasculare pentru combinația testată. În ansamblu, administrarea combinată de LB și SIL nu a indus citotoxicitate sau iritație suplimentară în comparație cu tratamentele individuale, susținând biosiguranța acestei asocieri.

Keywords: cardiovascular, cardiomyocyte, labetalol, silibinin

Introduction

Cardiovascular diseases (CVDs) remain the leading cause of mortality in both Europe and the United States, despite significant advances in medical care. Premature cardiovascular death is defined as occurring before the age of 70 years, with more than 60 million potential years of life lost annually across Europe due to these conditions (1).

The cardiovascular system includes the heart and blood vessels and can be affected by a wide range of conditions. CVDs are categorised into four main conditions: coronary artery disease (CAD), cerebrovascular disease, peripheral artery disease (PAD), and aortic atherosclerosis. Among these, CAD is the most prevalent, resulting from reduced myocardial perfusion and potentially leading to angina (chest pain), myocardial infarction, or heart failure. At the same time, the remaining entities are associated with stroke, limb ischemia, and aortic aneurysms (2).

Oxidative stress and inflammation are increasingly recognised as key mechanisms involved in the development and progression of cardiovascular diseases. Over the past decades, research has shown that an imbalance between reactive oxygen species and antioxidant defense systems contributes to vascular dysfunction and myocardial injury. These processes are important, especially in ischemic heart disease, where they are associated with the severity and clinical manifestations such as chest pain (angina pectoris) (3).

Angina pectoris occurs when the coronary arteries restrict blood flow, resulting in insufficient oxygen supply to the heart and causing ischemia. At the cellular level, this affects cardiomyocyte function and causes pain and myocardial stress (4). After myocardial infarction, interactions between cardiac oxidative stress and inflammatory cytokines have a major impact on cardiac contractility and clinical outcomes. Higher levels of oxidative stress markers and inflammatory mediators, such as tumor necrosis factor and interleukin-1 beta, are associated with lower cardiac function and a more unfavourable prognosis. In contrast, interventions that reduce oxidative and inflammatory responses may contribute to better improvement in cardiac performance (5). In addition to ischemic and inflammatory mechanisms, certain bacterial infections can affect the cardiovascular system, leading to severe complications such as infectious endocarditis, underscoring the sensitivity of cardiac tissues to inflammation-induced damage (6).

Pharmacological therapy remains the mainstay of cardiovascular disease management, including lipid-lowering agents, antihypertensive drugs, anti-thrombotic drugs, and antiarrhythmic drugs. However, the occurrence of drug-related adverse effects highlights the need for careful monitoring and individualised therapeutic approaches (7). In addition to drug therapy, palliative care can be a supportive approach that improves symptom management and the patient's overall well-being (8). In parallel, increasing attention has been directed toward natural bioactive compounds with cardioprotective potential, supporting their evaluation as complementary strategies alongside conventional treatments (7).

In this context, oxidative stress and inflammation are mechanisms involved in both the development and progression of cardiovascular diseases, especially myocardial ischemia and post-infarction cardiac dysfunction. Given the role of these processes in cardiomyocyte damage, compounds with antioxidant and anti-inflammatory properties have attracted significant interest as potential complementary strategies to standard pharmacological treatments.

Labetalol (LB) is an oral or intravenous antihypertensive that blocks α- and β-adrenergic receptors, lowering blood pressure, heart rate, and cardiac oxygen consumption. It is used in hypertension, angina, and myocardial ischemia and is considered safe during pregnancy. However, it can cause adverse reactions, which is why monitoring is required (9,10).

Silibinin (SIL) (11) is a flavonolignan derived from *Silybum marianum* and the main active component of silymarin, known in particular for its antioxidant properties. Experimental studies have shown that SIL reduces lipid peroxidation and oxidative stress *in vitro* and *in vivo*. In addition to its main antioxidant activity, SIL interferes with cellular signaling pathways involved in cell survival and apoptosis. Although these effects have been well studied in various pathologies, data on the impact of SIL on cardiac cells remain limited, which justifies the need to evaluate its safety profile in the cardiovascular context (12).

In vitro models are a practical experimental approach that allow evaluation of biosafety and cellular responses under controlled conditions, offering an optimal balance between biological relevance and experimental feasibility. The H9c2(2-1) cell line is a subclone of the original clonal cell line derived from embryonic BD1X rat heart tissue and exhibits several characteristics of skeletal muscle cells. Despite these features, H9c2(2-1) cells are commonly used in cardiovascular disease research as an *in vitro* model to investigate cardiomyocyte-related responses, including oxidative stress, ischemic injury, and drug-induced cardiotoxicity (13-15).

Previous studies have investigated the individual effects of LB and SIL using the H9c2(2-1) cardiomyocyte cell line. However, these studies are scarce, and data on the biosafety of their combined

administration remain limited. Therefore, the present study aimed to assess the *in vitro* and *in ovo* biosafety of LB and SIL, administered alone and in combination, using H9c2(2-1) cardiomyocyte cells and the chorioallantoic membrane (CAM) model..

Materials and Methods

Reagents and Instruments

Reagents obtained from Sigma-Aldrich (Merck KGaA, Darmstadt, Germany) included Dulbecco's Modified Eagle's Medium (DMEM), phosphate-buffered saline (PBS), Penicillin/Streptomycin, Silibinin, Labetalol, the MTT KIT, Acridine Orange, Propidium Iodide, and sodium lauryl sulfate (SLS). Hoechst 33342 nuclear stain and MitoTracker™ Red CMXRos were purchased from Thermo Fisher Scientific (Waltham, MA, USA). The measurements and imaging for the *in vitro* experiments were performed using a Cytation 5 multimode plate reader and a Lionheart FX automated microscope. At the same time, data acquisition and analysis were carried out with Gen5™ Microplate Data Collection and Analysis Software (version 3.14), provided by BioTek Instruments Inc. (Winooski, VT, USA), and Zeiss SteREO Discovery.V8 stereomicroscope used for the *in ovo* assay.

Cell Culture Conditions and Treatment Protocol

Experiments were performed using the immortalized myoblast cell line H9c2(2-1), obtained from the American Type Culture Collection (ATCC, Manassas, VA, USA). The cells were cultured in Dulbecco's Modified Eagle's Medium (DMEM) supplemented with 10% fetal bovine serum (FBS) and 1% penicillin–streptomycin solution. Cell cultures were maintained in a humidified incubator at 37 °C with 5% CO_2 throughout the experiments.

Stock solutions of LB and SIL were prepared in DMSO. From the stock solutions, five working dilutions were prepared for each substance and applied to H9c2(2-1) cells (LB: 20, 60, 120, 250, and 500 nM; SIL: 5, 25, 75, 100, and 200 µM). In addition, combined treatments were performed using LB + SIL at the following concentrations: 20 nM + 5 µM, 60 nM + 25 µM, 120 nM + 75 µM, 250 nM + 100 µM, and 500 nM + 200 µM. In all dilutions, the final DMSO concentration did not exceed 0.5% (v/v).

The LB concentrations used in this study were selected based on previously reported literature and were subsequently extended to cover a broader concentration range to enable a more comprehensive dose–response evaluation (10). Similarly, SIL concentrations were selected based on published studies and adapted to a 24 h exposure period, spanning a wide concentration range to assess dose-dependent cellular effects under the present experimental conditions (16).

Cell Viability Assessment Using the MTT Method

Cell viability was assessed using the MTT assay. H9c2(2-1) cells were seeded into 96-well plates at a density of 10.000 cells *per* well and maintained under standard culture conditions. After cell attachment, the cells were treated for 24 h with LB (20, 60, 120, 250, and 500 nM), SIL (5, 25, 75, 100, and 200 µM), and their combination (20 nM + 5 µM, 60 nM + 25 µM, 120 nM + 75 µM, 250 nM + 100 µM, and 500 nM + 200 µM). At the end of the treatment period, the culture medium was replaced with fresh medium, and 10 µL of MTT reagent was added to each well. The plates were then incubated for 3 h at 37 °C to allow the formation of formazan crystals. Subsequently, 100 µL of solubilization buffer *per* well was added, and the plates were kept at room temperature, protected from light, for 30 min. Absorbance was measured at 570 nm using a Cytation 5 microplate reader (BioTek Instruments Inc., Winooski, VT, USA).

Bright-Field Cell Morphology Analysis

Cell morphology was evaluated after 24 h of treatment with the tested compounds. H9c2(2-1) cells were exposed to LB (20, 60, 120, 250, and 500 nM), SIL (5, 25, 75, 100, and 200 µM), as well as to combined treatments at (20 nM + 5 µM, 60 nM + 25 µM, 120 nM + 75 µM, 250 nM + 100 µM, and 500 nM + 200 µM). Following the 24 h treatment period, cellular morphology was examined under bright-field microscopy to assess potential treatment-induced changes. Representative images were acquired using the Lionheart FX automated microscope and analysed with Gen5™ Microplate Data Collection and Analysis Software.

Neutral red (NR) assay

To further assess the lysosomal integrity, the Neutral Red uptake (NRU) assay was performed. The H9c2(2-1) cells were seeded into flat-bottom 96-well plates at a density of 10.000 cells *per* well and allowed to attach under standard culture conditions. Cells were then treated for 24 h with LB (20, 60, 120, 250, and 500 nM), SIL (5, 25, 75, 100, and 200 µM), as well as to combined treatments at (20 nM + 5 µM, 60 nM + 25 µM, 120 nM + 75 µM, 250 nM + 100 µM, and 500 nM + 200 µM). After the treatment period, the culture medium was removed and replaced with 100 µL of NR working solution *per* well (40 µg/mL NR in complete DMEM). The plates were incubated for 2 h at 37 °C in a humidified atmosphere containing 5% CO_2 to allow dye uptake by viable cells. Subsequently, the cells were gently washed with phosphate-buffered saline (PBS) to remove excess dye, and representative images were captured under bright-field illumination using a Lionheart FX automated microscope. For dye extraction, 150 µL of NR destaining solution (50% ethanol, 49% deionized water, and 1% glacial acetic acid) was added to each well, and the plates were

gently shaken for 10 min to ensure complete release of the dye from the cells. Absorbance was then measured at 540 nm using a Cytation 5 multimode plate reader.

Mitochondria and Nuclei Immunofluorescence Staining

To investigate potential mitochondrial and nuclear morphological changes, H9c2(2-1) cells were seeded into 12-well plates at a density of 100.000 cells *per* well and allowed to reach optimal confluence under standard culture conditions. Upon reaching the appropriate confluence, the cells were treated for 24 h with LB (20, 60, 120, 250, and 500 nM), SIL (5, 25, 75, 100, and 200 µM), or with their combination at the following concentrations: 20 nM + 5 µM, 60 nM + 25 µM, 120 nM + 75 µM, 250 nM + 100 µM, and 500 nM + 200 µM. Mitochondrial morphology was assessed using MitoTracker staining. A working solution of MitoTracker was prepared by diluting the stock solution in complete culture medium to obtain a final concentration of 300 nM. Cells were incubated with the staining solution for 30 min at 37 °C, then washed to remove excess dye. Subsequently, the cells were fixed with 4% paraformaldehyde for 10 min at room temperature and rinsed thoroughly with phosphate-buffered saline (PBS). Nuclear morphology was evaluated by staining the fixed cells with Hoechst 33342 (1:2000 dilution in PBS) for 5–10 min in the dark. After staining, the wells were washed three times with PBS. Representative images were captured using a Lionheart FX automated microscope, and image analysis was performed with Gen5™ Microplate Data Collection and Analysis Software (version 3.14; BioTek Instruments Inc., Winooski, VT, USA).

Acridine Orange/Propidium Iodide (AO/PI) Assay

To further evaluate the safety profile of the tested treatments at the cellular level, membrane integrity and viability were assessed using the Acridine Orange/Propidium Iodide (AO/PI) dual-staining assay. H9c2(2-1) cells were seeded in 96-well plates at a density of 10.000 cells *per* well and treated for 24 h with LB (20, 60, 120, 250, and 500 nM), SIL (5, 25, 75, 100, and 200 µM), and their combination (20 nM + 5 µM, 60 nM + 25 µM, 120 nM + 75 µM, 250 nM + 100 µM, and 500 nM + 200 µM). After this period, 100 µL of AO/PI staining solution prepared in complete culture medium (Acridine Orange, 10 µg/mL; Propidium Iodide, 10 µg/mL) was added to each well, and the plates were incubated at room temperature in the dark for 10 min. Fluorescence images were captured using a Lionheart FX automated microscope, and the staining patterns were interpreted with Gen5™ Microplate Data Collection and Analysis Software to qualitatively distinguish viable cells (AO-positive) from cells with compromised membranes (PI-positive).

Chorioallantoic Membrane (CAM) Model Preparation

Fertilized hen eggs were used for the chorioallantoic membrane (CAM) experiments. On day one, they were disinfected with ethanol, dated, and placed in an incubator for three days. On the fourth day, a small cut was made in the top of each one to remove approximately 7-8 mL of albumen using a syringe and needle. The cut was then sealed with adhesive tape. On the fifth day, the top of the shell was removed to expose the CAM blood vessels, after which the opening was resealed. The eggs were then returned to the incubator, where a temperature of 37 °C and 60% humidity were maintained until the experiments were performed.

Evaluation of Irritation Potential Using the HET-CAM Assay

Based on the *in vitro* concentration–response analysis, the combined treatment was further evaluated at the highest tested concentrations. The assay was performed on the tenth day of incubation. Purified distilled water was used as the negative control, and 1% sodium lauryl sulfate (SLS) as the positive control. A volume of 600 µL of each tested solution was carefully applied onto the chorioallantoic membrane. After application, vascular reactions, haemorrhage (H), lysis (L), and coagulation (C) were monitored for 5 minutes. Images of the membrane were captured both before exposure (T0) and 5 minutes post-application (T5) using a Zeiss Discovery V8 stereomicroscope equipped with an Axio CAM 105 camera. The acquired images were analysed using ZEN Core 3.8 software to evaluate changes in vascular integrity induced by each tested sample. The irritation score (IS), used to quantify the observed effects, was calculated according to the following formula:

$$IS = 5 \times \frac{301 - H}{300} + 7 \times \frac{301 - L}{300} + 9 \times \frac{301 - C}{300}$$

IS is used to evaluate the irritant potential of the tested samples by measuring the time-dependent appearance of vascular effects, including H, L, and C. Based on the resulting IS values, the tested substance is classified as follows: non-irritant for scores between 0 and 0.9, irritant for values ranging from 1 to 8.9, and severely irritant for scores between 9 and 21 (17).

Statistical Analysis

Data are presented as mean ± standard deviation (SD). The normality of data distribution was evaluated using the Shapiro–Wilk test. Since the data followed a normal distribution, statistical analyses were carried out using one-way analysis of variance (ANOVA), followed by Dunnett's multiple comparisons post hoc test. Statistical analysis was performed using GraphPad Prism software (version 10.2.3; GraphPad Software, San Diego, CA, USA). Differences were considered statistically significant at $*p < 0.05$, with increasing levels of significance

indicated as **p < 0.01, ***p < 0.001, and ****p < 0.0001. All experiments were performed in three independent biological replicates, each conducted in technical triplicate.

Results and Discussion

In the context of ischemic heart disease and angina pectoris, evaluating cellular and vascular biosafety is essential when considering combined pharmacological and antioxidant approaches. In light of this premise, the biosafety of LB and SIL, administered individually and in combination, was evaluated using an *in vitro* H9c2(2-1) cardiomyoblast model and an in ovo chorioallantoic membrane (CAM) assay to assess potential irritative effects.

Cell viability assessment in H9c2(2-1) cells following LB, SIL, and combined treatment

The first step of the study was to assess cell viability in H9c2(2-1) cells after 24 hours of treatment with LB, SIL, and their combination using the MTT assay. MTT is a colorimetric assay used to evaluate cellular metabolic activity and is one of the most commonly applied methods for assessing cell proliferation and viability *in vitro*. The assay is based on the ability of metabolically active cells to reduce the tetrazolium salt MTT to the insoluble purple formazan product *via* NAD(P)H-dependent oxidoreductase and dehydrogenase enzymes. This reduction occurs predominantly in the mitochondria of living cells, although enzymes located in other cellular compartments, such as the endoplasmic reticulum, may also contribute. The measured absorbance reflects the extent of intracellular MTT reduction and is commonly used as an indicator of cellular metabolic activity (18).

The results of this evaluation on H9c2(2-1) cells indicated that cellular viability was comparable to the control in nearly all samples after 24 h of treatment (Figure 1). Specifically, after 24 h treatment with LB, the following cell viability percentages were recorded: 101% at 20 nM, 100.66% at 60 nM, 99.33% at 120 nM, 99.13% at 250 nM, and 97.27% at 500 nM. For SIL treatment, cell viability at concentrations of 5, 25, 75, 100, and 200 µM was 102.67%, 98.63%, 98.58%, 95%, and 92.67%, respectively. Following combined treatment with LB and SIL (LB 20 nM + SIL 5 µM; LB 60 nM + SIL 25 µM; LB 120 nM + SIL 75 µM; LB 250 nM + SIL 100 µM; LB 500 nM + SIL 200 µM), the following cell viability percentages were obtained: 104.40%, 100%, 98.01%, 94.66%, and 91%, respectively.

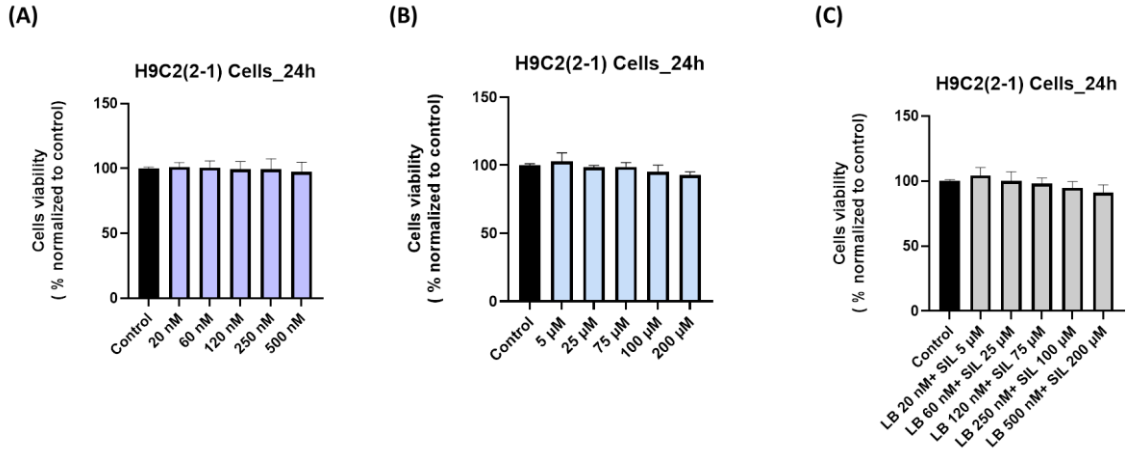

Figure 1.

Graphical representations of the effect induced by A) LB, B) SIL, and C) LB + SIL on H9c2(2-1) cell viability after 24h of treatment. The results are expressed as percentages normalised to control and are presented as mean values ± standard deviation. To evaluate the statistical differences between the control and treatment groups, a one-way ANOVA was conducted, followed by Dunnett's multiple comparison post hoc test. Statistical analysis revealed no significant differences between the control and treatment groups. The experiments were performed in triplicate

SIL was tested in another study on the H9c2(2-1) cell line at concentrations of 1, 10, 25, 50, and 100 µM using the MTT assay to assess cell viability. The results showed that all tested concentrations produced higher cell viability than the control, indicating that SIL did not have a cytotoxic effect on this cell line (16). Previous reports have shown that LB may induce a dose-dependent reduction in H9c2(2-1) cell viability following prolonged exposure (72 h) (8). In contrast, the present results demonstrate that short-term exposure (24 h) to LB, administered alone or in combination with SIL, does not adversely affect cell viability across a wide

concentration range (20–500 nM), supporting a favorable short-term biosafety profile.

Cell morphology analysis in H9c2(2-1) cells following LB, SIL, and combined treatment

The next step was to analyse the effects of LB, SIL, and their combination on the morphology of H9c2(2-1) cells after 24 hours of treatment. Cell morphology analysis is essential for identifying and classifying abnormalities, early cancer detection, and evaluating changes caused by environmental stressors. The results are quantitative, objective, and reliable, supporting diagnosis and the development of automated rapid analysis systems. In this context, cell morphology has become a fundamental field in image processing, aiming to quantitatively characterise cell structure and components to better understand the functioning and pathological processes associated with malignancy (19). Based on these considerations, morphological evaluation was further employed to assess the cellular response to the tested treatments. The results showed that none of the tested treatments had a toxic effect on the cells. At all concentrations investigated, the cells maintained their typical elongated morphology, similar to that of the control group. No significant morphological changes were observed, and cell confluence remained similar to that of the control group in all cases (Figure 2).

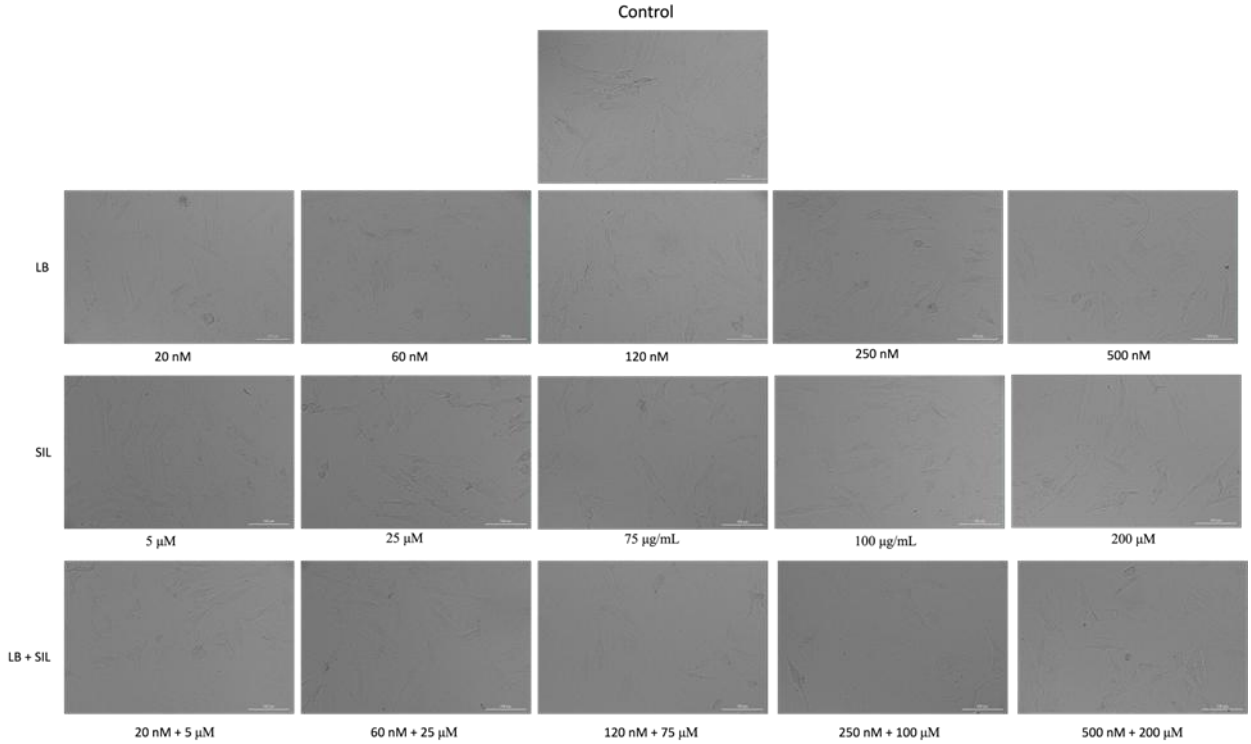

Figure 2.

The representative images show the morphological changes that were noticed in H9c2(2-1) cells after 24 hours of treatment with LB (20, 60, 120, 250, and 500 nM), SIL (5, 25, 75, 100, and 200 µM), as well as to combined treatments at (20 nM + 5 µM, 60 nM + 25 µM, 120 nM + 75 µM, 250 nM + 100 µM, and 500 nM + 200 µM) The scale bar indicates 100 µm. The experiments were performed in triplicate

Similarly, in a study by Dehelean *et al*., the impact of SIL at 100 µM on the morphological characteristics of H9c2(2-1) cells was evaluated. The results showed that, after 24 hours of treatment, SIL did not cause significant morphological changes compared to the control, with similar cell morphology and confluence, indicating the absence of a cytotoxic effect at this concentration (16).

Lysosomal integrity assessment in H9c2(2-1) cells by neutral red uptake assay

Because the MTT assay generally reflects cellular viability based on metabolic activity and, thereby, mitochondrial function, the NRU assay was performed to evaluate cellular viability through a complementary mechanism. This assay primarily reflects lysosomal integrity following treatment (20). The results of the NRU assay (Figure 3) indicated that NRU levels remained similar to the control in all samples, suggesting preservation of lysosomal integrity.

Quantitative analysis (Figure 4) revealed the following NRU values after treatment with LB at concentrations of 20, 60, 120, 250, and 500 nM: 99.33%, 97%, 96.67%, 95.67%, and 95%, respectively. Following SIL treatment at concentrations of 5, 25, 75, 100, and 200 µM, the observed NRU

values were 101.68%, 101.32%, 95.54%, 91.67%, and 90.30%, respectively. Combined treatment with LB and SIL (LB 20 nM + SIL 5 μM; LB 60 nM + SIL 25 μM; LB 120 nM + SIL 75 μM; LB 250 nM + SIL 100 μM; LB 500 nM + SIL 200 μM) resulted in NRU values of 99.48%, 98.55%, 91.72%, 89.25%, and 86.89%, respectively.

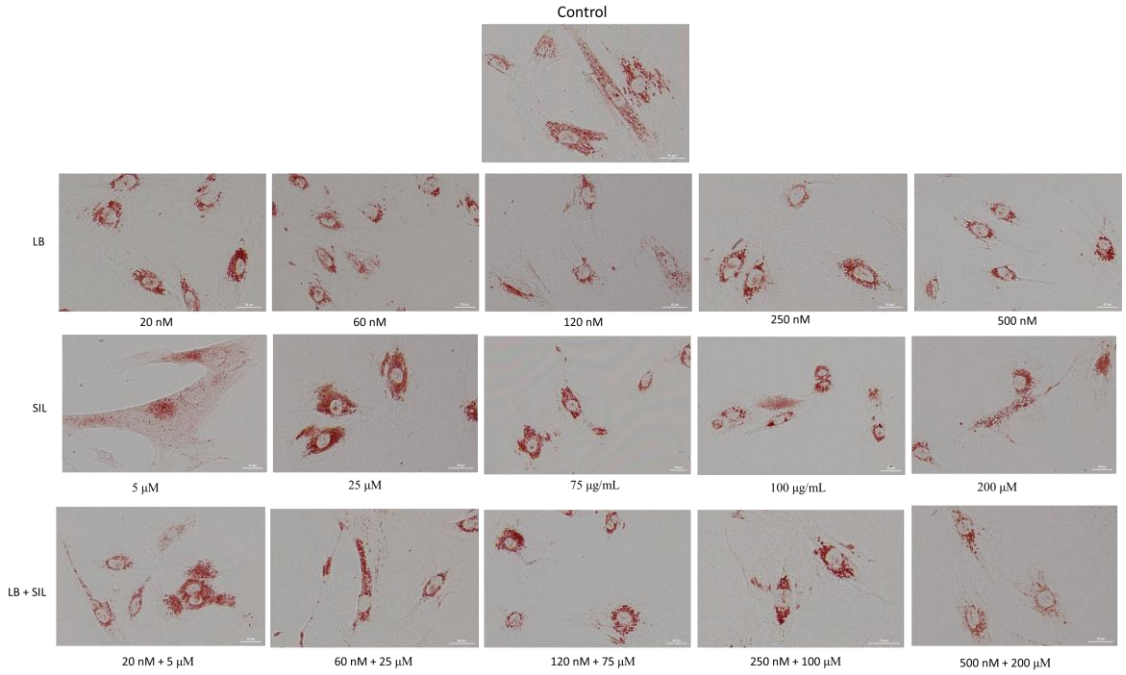

Figure 3.
The Neutral Red Uptake of H9c2(2-1) cells after 24h exposure to LB, SIL, and their combinations after 24 h of treatment. The scale bar indicates 30 μm. The experiments were performed in triplicate

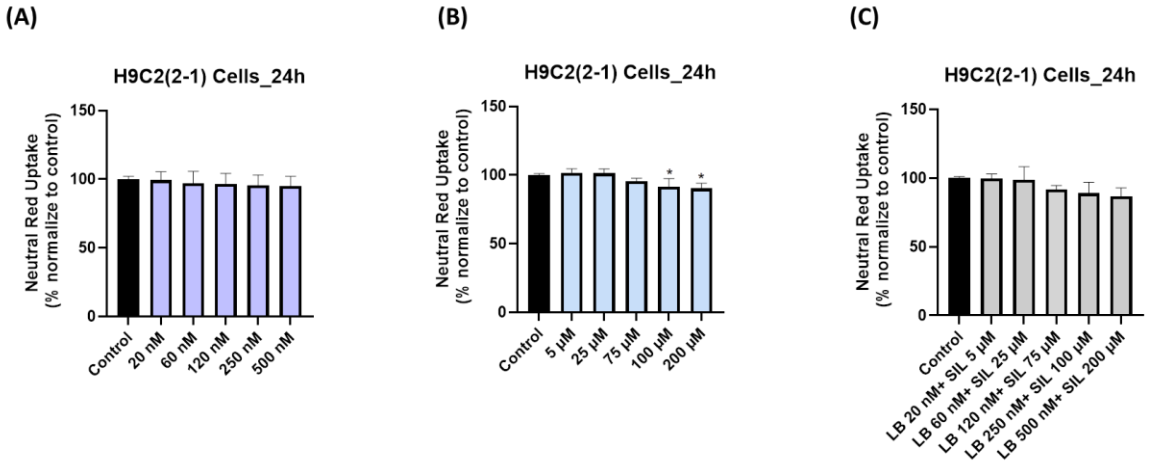

Figure 4.
Graphical representations of the effect induced by A) LB, B) SIL, and C) LB + SIL on H9c2(2-1) Neutral Red Uptake level after 24 h of treatment. The results are expressed as percentages normalised to control and are presented as mean values ± standard deviation. To evaluate the statistical differences between the control and treatment groups, a one-way ANOVA was conducted, followed by Dunnett's multiple comparison post hoc test. Statistical analysis revealed no significant differences between the control and treatment groups. "*" indicates statistical significance *$p < 0.05$ The experiments were performed in triplicate

Lysosomes are cellular organelles equipped with an enzymatic system composed of a wide range of enzymes (approximately 50) that play an important role in the cellular catabolism of molecules such as proteins, lipids, DNA and RNA, as well as carbohydrates. In addition to their key involvement in essential cellular processes such as endocytosis, autophagy, and phagocytosis. Therefore, lysosomes

have a key role in maintaining cellular homeostasis (21). At the level of cardiomyocytes, which are post-mitotic (they do not divide), lysosomes play a critical role in maintaining their functional integrity. In this context, lysosomes contribute to the removal of cellular debris such as oxidized proteins, protein aggregates, and dysfunctional or damaged organelles, including mitochondria. Any impairment of lysosomal function leads to the accumulation of these "waste" products, increased oxidative stress, and defects in cellular bioenergetics due to reduced ATP production**,** which are accompanied by the activation of apoptotic processes in cardiomyocytes. These alterations result in disturbances of cardiac cell function and predispose cardiac tissue to pathological conditions such as ischemia and heart failure, while also promoting accelerated aging of the myocardium (22). In light of these considerations, lysosomal integrity is a relevant endpoint in cytotoxicity studies of cardiomyocytes. In the present study, the assessment of lysosomal preservation was performed using the Neutral Red Uptake NRU assay. The NRU assay is a commonly used method for determining cell viability by measuring the pH-dependent accumulation of the Neutral Red dye within lysosomes. Thus, at physiological pH, the cationic reagent penetrates the cell membrane *via* passive, nonionic diffusion and binds to anionic groups within lysosomes. At the same time, the binding capacity of NR at the lysosomal level is considered an indicator of cell viability (20). Nevertheless, the Neutral Red assay has also been reported in the literature for H9c2(2-1) cells as a complementary approach to the MTT assay to further investigate cell viability and cytotoxicity. For example, Arbo *et al*. (23) employed a similar approach, evaluating the cytotoxic potential of various piperazine derivatives on these cells after 24 hours of treatment at concentrations ranging from 0 to 20 mM. In addition, phytocompounds such as quercetin (at concentrations of 5–25 µM) and 2,3-dehydrosilybin (at concentrations of 2–10 µM), which are structurally related to SIL, have also been tested on this cell line by Dostál *et al*. to determine their protective effects on cardiomyocytes against osmotic stress induced by hypertonic treatment. It was observed that both compounds improved these cells' tolerance to stress conditions (24). Furthermore, Misiak and his collaborators investigated the effects of doxorubicin-loaded polymeric nanoparticles at a concentration range of 0.05 - 0.5 mg/mL on cell biocompatibility after 24h of exposure using the NRU assay (25). Similarly, Szymczuk *et al*. evaluated the cytotoxicity of iron oxide nanoparticles in H9c2(2-1) cells after 24 h of exposure at 0.1 mg/mL (26).

Immunofluorescence-based evaluation of mitochondrial and nuclear morphology in H9c2(2-1) cells

To further evaluate the cellular effects of the treatments, mitochondrial and nuclear morphology were assessed using specific fluorescent staining. As shown in Figure 5, analysis performed 24 hours after treatment with SIL, LB, and their combination revealed that nuclear and mitochondrial characteristics remained comparable to those of the control group. The mitochondria showed a well-preserved reticular organisation, with a predominance of elongated shapes and only minor changes in fluorescence intensity. Similarly, the nuclei remained uniform and regular in shape, comparable to those of untreated cells.

â

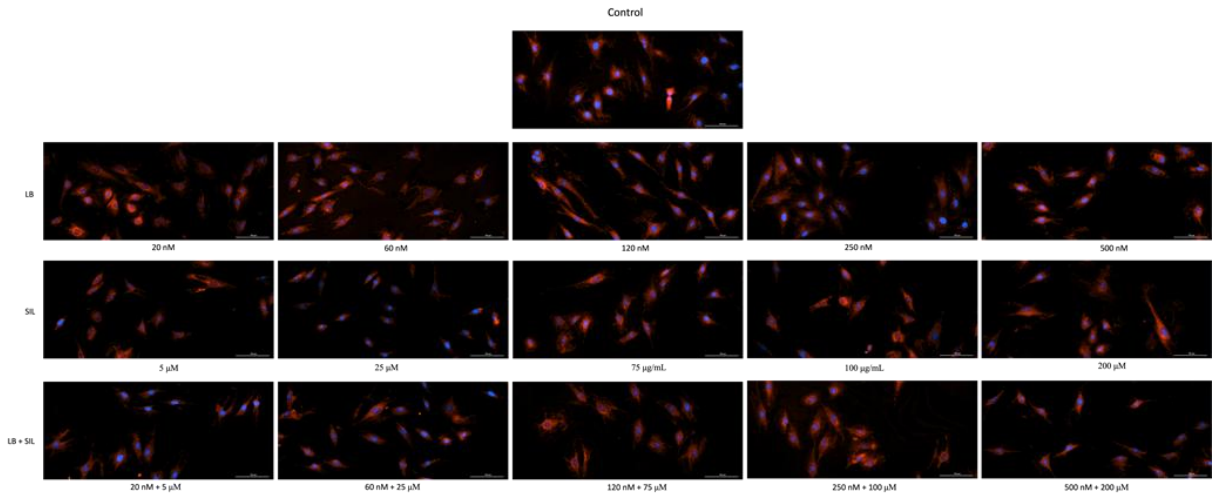

Figure 5.

Representative images of the impact of LB, SIL, and their combination after 24 h of treatment on mitochondria and nuclei morphology in H9c2(2-1) cells. The scale bar indicates 100 µm. The experiments were performed in triplicate

The detection of apoptosis is critical to evaluating the antitumor potential of therapeutic agents, as programmed cell death enables the selective removal of cancer cells while sparing normal tissues. Fluorescence microscopy combined with Hoechst 33342 staining is a widely used approach for identifying apoptosis-related nuclear alterations, including chromatin condensation and nuclear fragmentation. Hoechst 33342 binds to DNA and emits blue fluorescence, allowing clear visualisation of nuclear morphology. This technique is commonly applied *in vitro* to distinguish between viable, apoptotic, and necrotic cells (17). Another approach to assessing apoptosis is to evaluate mitochondrial membrane potential using mitochondrial potential-dependent staining. During the early stages of apoptosis, a decrease in mitochondrial membrane potential occurs before pronounced morphological changes, making this method a sensitive indicator of functional alterations in cells. This type of analysis allows the identification of cells with preserved mitochondrial activity and helps distinguish non-apoptotic cells from those undergoing programmed cell death (27). SIL (100 µM) was evaluated at 24 h on the H9c2(2-1) cell line by Hoechst 33342 staining to assess any possible changes in cell nuclei morphology. The results showed that it did not induce significant changes in cell nuclei; these findings are consistent with those obtained in the present study, both for SIL administered individually and for the combinations evaluated (16).

Assessment of the potential apoptotic and necrotic effects in H9c2(2-1) cells by acridine orange/ propidium iodide staining

Microscopic evaluation using acridine orange/ propidium iodide (AO/PI) staining, performed to assess the treatments' potential to induce apoptotic or necrotic cellular alterations, revealed the following (Figure 6). After treatment with LB, a predominantly green, diffuse fluorescence pattern was observed in H9c2(2-1) cells up to 250 nM, with no evident morphological features of apoptosis or necrosis. At 500 nM LB, a very small proportion of cells exhibited red fluorescence indicative of cellular necrosis, as evidenced by propidium iodide uptake. In response to SIL treatment, H9c2(2-1) cells showed early apoptotic features, such as membrane blebbing and chromatin condensation, at the highest tested concentration (200 µM). Nevertheless, green fluorescence remained predominant and comparable to the control condition, indicating that overall cell viability was preserved. In the case of combined treatment, sporadic red fluorescent cells suggestive of necrosis were detected at the combinations of LB 250 nM + SIL 100 µM and LB 500 nM + SIL 200 µM; however, these events were observed at a very low frequency. Overall, these observations demonstrate that neither LB nor SIL, alone or in combination, significantly promotes apoptotic or necrotic cell death in H9c2(2-1) cells under the present experimental conditions.

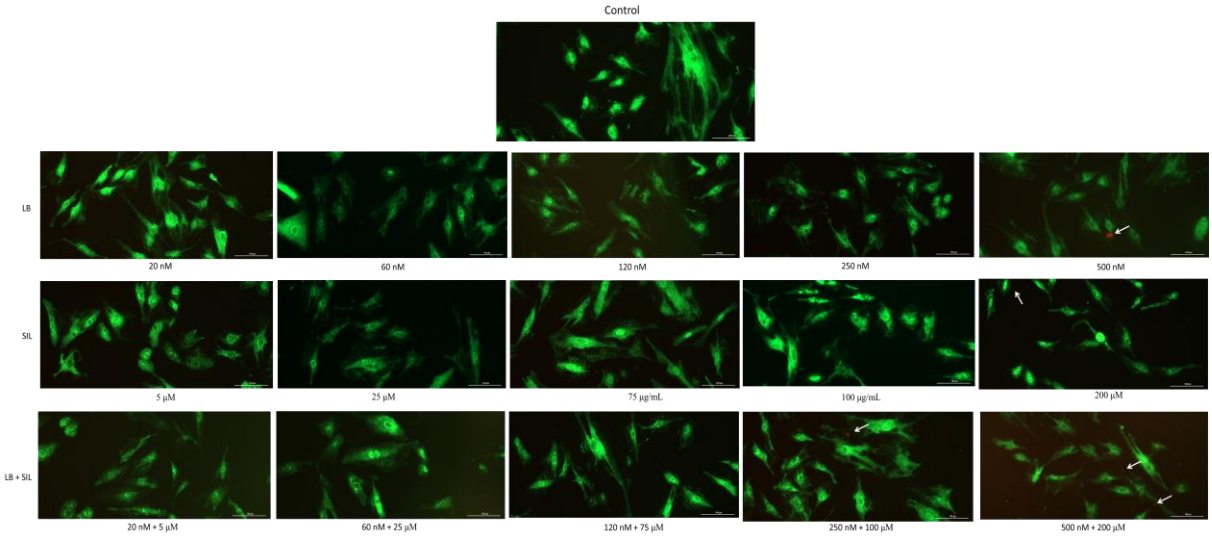

Figure 6.

Representative images of the impact of LB, SIL, and their combinations after 24 h in H9c2(2-1) cells stained with AO/PI. The white arrows indicate signs of necrosis (red fluorescence), chromatin condensation, or cell blebbing. The scale bar indicates 100 µm. The experiments were performed in triplicate

Additionally, to further assess the potential apoptosis or necrosis effect of samples using the acridine orange/propidium iodide (AO/PI) assay in H9c2(2-1) cells. AO/PI is a fluorescence-based technique used to evaluate cell viability as well as apoptotic and necrotic cell death. AO permeates all cells and binds to nucleic acids, staining viable cells with green fluorescence in the nucleus and cytoplasm. In

contrast, PI enters only cells with compromised membrane integrity, labelling them with red fluorescence. This dual-staining approach allows differentiation between viable, apoptotic, and necrotic cells (28). However, this assay has also been used in other studies to assess the apoptosis-inducing potential and effects on cell viability of H9c2(2-1) cells when exposed to various compounds, as an additional approach to safety evaluation. For example, Mohan *et al*. investigated the effects of *Catha edulis* extract on H9c2(2-1) cells within a concentration range of 0–100 µg/mL at different time points (24, 48, and 72 h). Early signs of apoptosis, such as changes in green fluorescence patterns, chromatin condensation, and cell blebbing, were observed between 24 and 48 h. At 72 h, features of necrosis were also detected, indicated by the appearance of PI-positive cells exhibiting red fluorescence (29). Also, Yuvaraj *et al.* evaluated the protective effect of chrysin, a flavonoid, at concentrations of 5–100 µM in this cell line. The cells were pretreated with chrysin for 24 hours and subsequently exposed to H_2O_2-induced oxidative stress. The results of this assay indicated that chrysin reduced the toxic and necrotic effects caused by H_2O_2 exposure, as evidenced by a decrease in red fluorescence intensity (30). Moreover, this assay is commonly used in studies evaluating the safety profile of SIL on normal cells. For example, Vakili *et al*. employed this method to assess the effects of SIL on human umbilical vein endothelial cells (HUVEC) at concentrations ranging from 0 to 200 µg/mL over different time points (24, 48, and 72 h). Their results showed that SIL induced marked necrosis, as evidenced by the predominant appearance of red fluorescence in the treated cell population (31).

Evaluation of Irritation Potential Using the HET-CAM Assay

The irritant potential of the highest tested concentration of the LB and SIL combination (500 nM + 200 µM) was evaluated using the HET-CAM assay. The chorioallantoic membrane (CAM) of the chick embryo is a widely used experimental model for irritation testing, recognised as a rapid, simple, and cost-effective technique. This method does not require stringent ethical approval, as the chick embryo is not classified as a live animal before day 17 of development (32).

In this study, the HET-CAM test was used to evaluate the irritant potential of the LB-SIL combination. Distilled water was used as a negative control, and 1% sodium lauryl sulfate (SLS) as a positive control. The appearance of characteristic vascular changes, such as hemorrhage, lysis, and coagulation, was monitored for 5 minutes, and the irritation score (IS) was determined based on the time of occurrence of these changes. The results (Figure 7 and Table I) showed that neither the LB + SIL combination nor distilled water induced changes in the chorioallantoic membrane. The blood vessels remained intact, with no visible changes, similar to the negative control, indicating the absence of an irritant effect and classifying it as a non-irritating substance (IS = 0.07). In contrast, 1% SLS caused the rapid appearance of all specific signs of irritation, with a high irritation score (IS = 18.32), classifying it as a severely irritating substance (33).

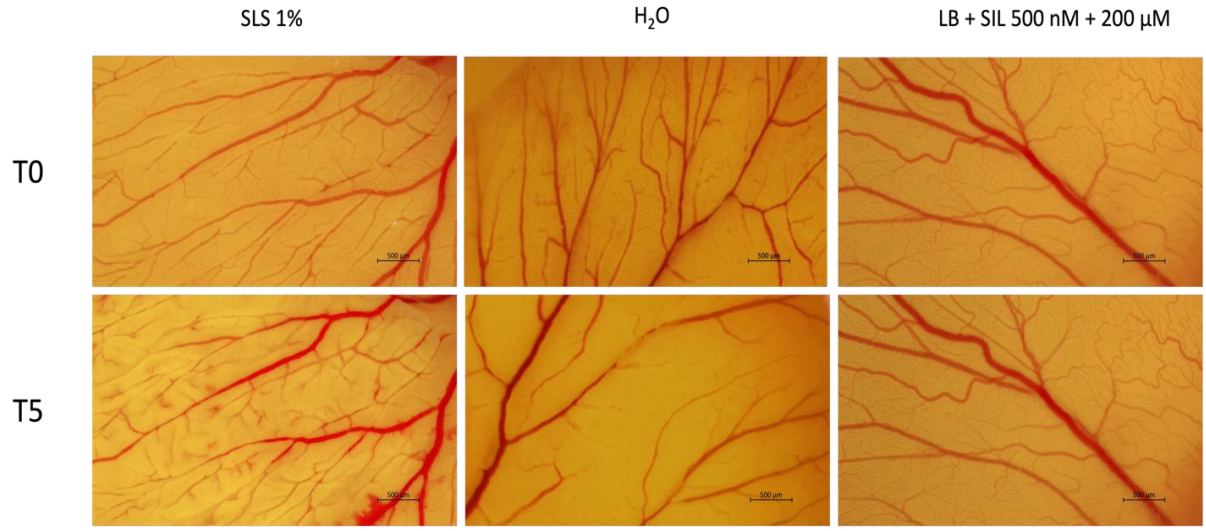

Figure 7.
Stereomicroscope images of the CAMs treated with sodium lauryl sulfate 1%—SLS used as positive control, H2O used as negative control, and LB + SIL (500 nM + 200 µM), before (T0) and five minutes (T5) post-treatment. Scale bars indicate 500 µm

Table I

Irritation score values for positive control (SLS 1%), negative control (distilled water), and LB + SIL 500 nM + 200 μM

Sample	Irritation score (IS)	Irritation category
SLS 1%	18,32	Severe irritant
H_2O	0,070	Non-irritant
LB + SIL (500 nM + 200 μM)	0,070	Non-irritant

Conclusions

Cardiovascular diseases, including ischemic heart disease and angina pectoris, remain a major cause of morbidity and mortality worldwide, with oxidative stress and inflammation playing a central role in myocardial injury and disease progression. In this context, evaluating the biosafety of both conventional pharmacological agents and complementary compounds is essential.

In the present study, the biosafety profiles of LB, SIL, and their combined administration were investigated using complementary *in vitro* and *in ovo* experimental models. The results demonstrated that neither individual nor combined treatments induced significant cytotoxic effects in H9c2(2-1) cells, as cell viability remained high and nuclear and mitochondrial morphology was preserved. Moreover, the CAM assay confirmed the absence of irritant or vascular-damaging effects associated with the LB and SIL combination, supporting good cellular and vascular tolerability. Despite these promising results, some limitations should be considered. The study was limited to *in vitro* and *in ovo* models and focused mainly on biosafety and morphological endpoints, without evaluating functional cardiac outcomes. Future studies should further explore the underlying cellular mechanisms and assess the effects of LB and SIL in more complex, disease-relevant models of myocardial ischemia and angina pectoris.

Acknowledgement

The authors would like to thank "Victor Babeș" University of Medicine and Pharmacy Timișoara for supporting the experimental activities conducted in this study.

Funding

Not applicable.

Availability of data and materials

The data generated in the present study are included in the figures and/or tables of this article.

Ethics

Not applicable

AI use disclosure

During the preparation of this manuscript, the authors used QuillBot for language improvement, including spelling, grammar, clarity, and readability. The authors reviewed and revised all outputs from these tools and take full responsibility for the final content of the work.

Conflict of interest

The authors declare no conflict of interest.

References

1. Morariu Briciu DM, Bolintineanu SL, Rata A, Semenescu AD, Anton A, Jijie R, et al. Assessment of the biosafety profile of Galium verum in vitro on myoblasts and in ovo on chorioallantoic membrane. World J Cardiol. 2025;17(2):102310.
2. Olvera Lopez E, Ballard BD, Jan A. Cardiovascular Disease [online]. Treasure Island (FL): StatPearls Publishing; 2023 [cited 2026 Jan 10]. Available from: https://www.ncbi.nlm.nih.gov/books/NBK535419/
3. Kibel A, Lukinac AM, Dambic V, Juric I, Selthofer Relatic K. Oxidative Stress in Ischemic Heart Disease. Oxid Med Cell Longev. 2020;2020(1):6627144.
4. Crossman DC. The pathophysiology of myocardial ischaemia. Heart. 2004;90(5):576-580.
5. Duan D, Li H, Chai S, Zhang L, Fan T, Hu Z, et al. The relationship between cardiac oxidative stress, inflammatory cytokine response, cardiac pump function, and prognosis post-myocardial infarction. Sci Rep. 2024;14(1):8985.
6. Stroescu RF, Chisavu F, Steflea RM, Doros G, Bizerea-Moga TO, Vulcanescu DD, et al. A Retrospective Analysis of Systemic Bartonella henselae Infection in Children. Microorganisms. 2024;12(4):666.
7. Netala VR, Teertam SK, Li H, Zhang Z. A Comprehensive Review of Cardiovascular Disease Management: Cardiac Biomarkers, Imaging Modalities, Pharmacotherapy, Surgical Interventions, and Herbal Remedies. Cells. 2024;13(17):1471.
8. Hizanu-Dumitrache M, Boeriu E, Tanasescu S, Balan A, Oprisoni LA, Popa MV, et al. Benefits of Respite Services on the Psycho-Emotional State of Families of Children Admitted to Hospice Palliative Care Unit: Preliminary Study on Parents' Perceptions. Healthcare. 2024;12(7):748
9. Abdullah A, Yusof MK. Labetalol: A Brief Current Review. Pharmacophore. 2019;10(6): 50-56.
10. Rednic R, Marcovici I, Dragoi R, Pinzaru I, Dehelean CA, Tomescu M, et al. In vitro Toxicological Profile of Labetalol-Folic Acid/Folate Co-Administration in

H9c2(2-1) and HepaRG Cells. Medicina. 2022;58(6):784.
11. PubChem. PubChem Compound Summary for CID 31553, Silibinin [online]. Bethesda (MD): National Library of Medicine (US), National Center for Biotechnology Information; 2004 [cited 2026 Jan 10]. Available from: https://pubchem.ncbi.nlm.nih.gov/compound/Silibinin
12. Anestopoulos I, Kavo A, Tentes I, Kortsaris A, Panayiotidis M, Lazou A, et al. Silibinin protects H9c2 cardiac cells from oxidative stress and inhibits phenylephrine-induced hypertrophy: potential mechanisms. J Nutr Biochem. 2013;24(3):586-594.
13. American Type Culture Collection. H9c2(2-1) rat cardiomyoblast cell line (ATCC® CRL-1446™) [online]. Manassas (VA): ATCC; 2024 [cited 2026 Jan 19]. Available from: https://www.atcc.org/products/crl-1446.
14. Zhang L, Liu L, Li X, Zhang X, Zhao J, Luo Y, et al. TRAP1 attenuates H9C2 myocardial cell injury induced by extracellular acidification via the inhibition of MPTP opening. Int J Mol Med. 2020;46(2):663-674.
15. Liu F, Zhang H, Li Y, Lu X. Nobiletin suppresses oxidative stress and apoptosis in H9c2 cardiomyocytes following hypoxia/reoxygenation injury. Eur J Pharmacol. 2019;854:48-53.
16. Dehelean C, Alexa E, Marcovici I, Iftode A, Lazar G, Simion A, et al. Synthesis, characterization, and in vitro–in vivo toxicological screening of silibinin fatty acids conjugates as prodrugs with potential biomedical applications. Biomol Biomed. 2024;24(6):1735-1750.
17. Romînu R, Iftode OA, Boța M, Predescu IA, Jijie AR, Vlaia L, et al. Assessment of the antitumour potential of Melissa officinalis ethanolic extract on A375 melanoma cells: in vitro and in ovo approaches. Farmacia. 2025;73(3):737-747.
18. Kuete V, Karaosmanoğlu O, Sivas H. Anticancer Activities of African Medicinal Spices and Vegetables. In: Kuete V. Medicinal Spices and Vegetables from Africa; Elsevier: Amsterdam, The Netherlands; 2017. pp. 271-297.
19. Chen S, Zhao M, Wu G, Yao C, Zhang J. Recent advances in morphological cell image analysis. Comput Math Methods Med. 2012:101536.
20. Repetto G, del Peso A, Zurita J. Neutral red uptake assay for the estimation of cell viability/cytotoxicity. Nat Protoc. 2008;3(7):1125-1131.
21. Cooper GM. Lysosomes. The Cell: A Molecular Approach. 2nd ed. Sunderland (MA): Sinauer Associates; 2000.
22. Terman A, Kurz T, Gustafsson B, Brunk UT. The involvement of lysosomes in myocardial aging and disease. Curr Cardiol Rev. 2008;4(2):107-115.
23. Arbo MD, Silva R, Barbosa DJ, Dias da Silva DD, Rossato LG, Bastos ML, et al. Piperazine designer drugs induce toxicity in cardiomyoblast H9c2 cells through mitochondrial impairment. Toxicol Lett. 2014;229(1):178-189.
24. Dostál Z, Zholobenko AV, Přichystalová H, Gottschalk B, Valentová K, Malli R, et al. Quercetin protects cardiomyoblasts against hypertonic cytotoxicity by abolishing intracellular Ca^{2+} elevations and mitochondrial depolarisation. Biochem Pharmacol. 2024;222:116094.
25. Misiak P, Niemirowicz-Laskowska K, Markiewicz KH, Wielgat P, Kurowska I, Czarnomysy R, et al. Doxorubicin-loaded polymeric nanoparticles containing ketoester-based block and cholesterol moiety as specific vehicles to fight estrogen-dependent breast cancer. Cancer Nanotechnol. 2023;14(1):23.
26. Szymczuk D, Markiewicz KH, Niemirowicz-Laskowska K, Sawicka D, Misztalewska-Turkowicz I, Car H, et al. Covalent modification of iron oxide-poly (lithocholic acid) nanoparticles with folic acid or doxorubicin – an approach for enhanced cancer therapy. RSC Adv. 2025;15(18):14246-14258.
27. Barteneva NS, Ponomarev ED, Tsytsykova A, Armant M, Vorobjev IA. Mitochondrial staining allows robust elimination of apoptotic and damaged cells during cell sorting. J Histochem Cytochem. 2014;62(4):265-275.
28. Hussain H, Raj LS, Ahmad S, Abd Razak MF, Wan Mohamud WN, Bakar J, et al. Determination of cell viability using acridine orange/propidium iodide dual-spectrofluorometry assay. Cogent Food Agric. 2019;5(1):1582398.
29. Mohan S, Abdelwahab SI, Hobani YH, Syam S, Al-Zubairi AS, Al-Sanousi R, et al. Catha edulis extract induces H9c2 cell apoptosis by increasing reactive oxygen species generation and activation of mitochondrial proteins. Pharmacogn Mag. 2016;12(3):321-326.
30. Yuvaraj S, Ajeeth AK, Puhari SSM, Abhishek A, Ramprasath T, Vasudevan V, et al. Chrysin protects cardiac H9c2 cells against H_2O_2-induced endoplasmic reticulum stress by up-regulating the Nrf2/PERK pathway. Mol Cell Biochem. 2023;478(3):539-553.
31. Vakili-Zahir N, Nakhjavani M, Hajian P, Shirazi FH, Mirzaei H. Evaluation of silibinin effects on the viability of HepG2 (human hepatocellular liver carcinoma) and HUVEC (human umbilical vein endothelial) cell lines. Iran J Pharm Res. 2018;17(1):261-267.
32. Sirbu MI, Predescu IA, Horhat DI, Mot IC, Banta AM, Orășan A, et al. Evaluation of quercetin, myricetin and their combination as flavonoids with antitumour potential in head and neck cancer models: an in vitro and in ovo study. Farmacia. 2025;73(5):1143-1154.
33. Leoty-Okombi S, Gillaizeau F, Leuillet S, Douillard B, Le Fresne-Languille S, Carton T, et al. Effect of Sodium Lauryl Sulfate (SLS) Applied as a Patch on Human Skin Physiology and Its Microbiota. Cosmetics. 2021; 8(1):6.